Presented at the 42nd IEEE Photovoltaic Specialist Conference, 14-19 June 2015, New Orleans, United States of America

Evaluation of Screen-Printed Metallization Concepts for Large-Area BC-BJ Solar Cells

Max Hendrichs[1], Milan Padilla[1], Johann Walter[1], Florian Clement[1], Andreas Fell[2], Bernd Rech[3]

[1]Fraunhofer Institute for Solar Energy Systems ISE, Heidenhofstraße 2, 79110 Freiburg, Germany,
[2]College of Engineering and Computer Science, ANU, Canberra, A.C.T. 0200, Australia
[3]Helmholtz Center Berlin for Materials and Energy, Kekuléstraße. 5, 12489 Berlin, Germany

***Abstract* — In this study, we investigate a wire-based interconnection approach for back-contact back-junction (BC-BJ) solar cells with an edge length of 156 mm and screen-printed contact finger metallization. Every second contact finger is interrupted periodically, hence allowing for connecting contact fingers of each single polarity by wires without an additional insulation layer. By means of numerical simulations using the software *Quokka*, we show that contact finger interruptions up to 1 mm have no significant negative impact on the cell performance ($\Delta\eta < 0.1\ \%_{abs}$). Furthermore, adhesion tests of soldered cell interconnectors are carried out for different metallization concepts, aiming at finding suitable solder pad dimensions for 156 mm BC-BJ solar cells. Peel forces exceeding 1 N/mm are found for both investigated metallization concepts with i) screen-printed copper-based busbars with screen-printed insulation layer beneath, and ii) wire-based busbars without insulation layer.**

***Index Terms* — back-contact, metallization, module integration, screen printing, silicon.**

I. Introduction

Back-contact back-junction (BC-BJ) solar cells are known for their superior conversion efficiency potential both on cell and module level [1]. Today, almost all industrially produced BC-BJ solar cells feature a wafer edge length of 125 mm with two rear busbars, each located at opposed wafer edges [2]. A major challenge in transferring the cell concept to wafers with an edge length of 156 mm is to keep resistive losses, caused by the cell metallization, on an acceptable low level. The adaption of the edge busbar metallization layout seems to be unsuitable for this purpose, since the contact finger length increases significantly and, therefore, a higher contact finger cross-section is needed. This increased requirement can be hardly achieved with industrial screen printing technology, hence alternative metallization concepts have to be investigated for 156 mm BC-BJ solar cells with screen-printed contact finger metallization.

In this study we compare two different metallization concepts for large-area BC-BJ solar cells based on screen printing that allow for low series resistance contribution of the cell metallization.

The first concept, shown in Fig. 1a, is based on a multi-layer metallization approach [3, 4] where the busbar metallization is decoupled from the contact finger metallization by an intermediate insulation layer. It is compatible with ribbon- or foil-based module integration technologies and consists of three consecutively screen-printed layers: the contact finger metallization, the insulation layer, and the busbar metallization.

The second concept, shown in Fig. 1b, is compatible with wire-based interconnection approaches such as “Multi Busbar” [5] or “SmartWire” [6]. The cell metallization consists solely of screen-printed contact fingers that feature periodic interruptions thus allowing for interconnecting contact fingers of one polarity using wires [7]. Compared with the multi-layer

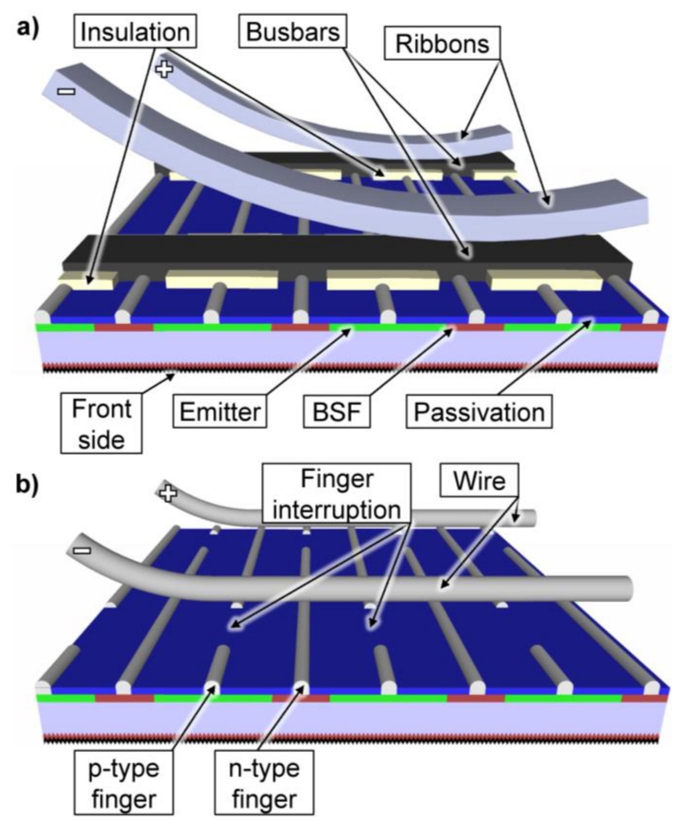

Fig. 1. Schematic cross sections of the investigated BC-BJ metallization concepts: a) multi-layer concept with intermediate insulation layer; b) wire-based concept with periodic contact finger interruptions.

metallization concept, two screen printing processes can be omitted at the end of the cell manufacturing. However, the periodic contact finger interruption might cause a reduction of the cell conversion efficiency due to increased lateral current paths in the doped layers on the cell rear. The major challenge of the wire-based metallization approach is the optimization of the contact layout. On the one hand the contact finger interruption must be wide enough to ensure a reliable cell interconnection process in an industrial-like production environment. On the other hand it should be as small as possible in order to avoid significant cell performance losses.

In the following, we quantify the influence of the contact finger interruption width on the performance of BC-BJ solar cells with wire-based metallization concept by means of numerical simulations. In addition, we present a detailed adhesion force study for both investigated BC-BJ metallization concepts with soldered cell interconnectors. The shape and the area of the external contact pads are varied systematically in order to find suitable external contact pad dimensions for both metallization concepts.

TABLE I

INPUT PARAMETERS FOR THE QUOKKA SIMULATION OF N-TYPE CZ-SI BC-BJ SOLAR CELLS.

Parameter	Unit	Input
Wafer thickness W	µm	180
Wafer edge length l_{cell}	mm	156
Pitch p	mm	1.5
Emitter width d_E	µm	1200
BSF width d_{BSF}	µm	300
Contact width d_C	µm	50
Emitter sheet resistance $R_{SH,E}$	Ω/sq	65
BSF sheet resistance $R_{SH,BSF}$	Ω/sq	40
FSF sheet resistance $R_{SH,FSF}$	Ω/sq	235
Base resistivity ρ_B	Ωcm	3
Emitter dark saturation current density $j_{0,E}$	fA/cm²	30
BSF dark saturation current density $j_{0,BSF}$	fA/cm²	130
FSF dark saturation current density $j_{0,FSF}$	fA/cm²	43
Dark saturation current density of the metallized emitter $j_{0met,E}$	fA/cm²	1500
Dark saturation current density of the metallized BSF $j_{0met,BSF}$	fA/cm²	800
Contact resistivity ρ_C	mΩcm²	3
Line resistivity of contact finger R_L	Ω/m	100
Specific resistivity of copper wire ρ_{wire}	µΩcm	5
Radius of copper wire r_{wire}	µm	125

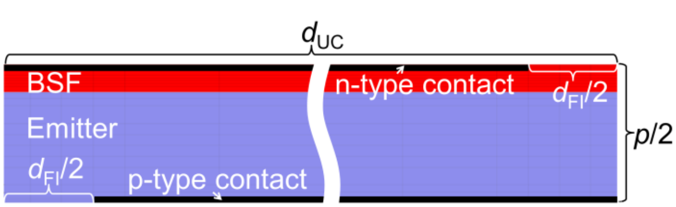

Fig. 2. Schematic of the unit cell simulated using *Quokka* (topview of the cell rear). The width of the unit cell d_{UC} and the width of the contact finger interruption d_{FI} are varied systematically.

II. APPROACH

A. Simulation of Wire-Based Cell Metallization Layouts

In order to quantify the effect of the contact finger interruption on the current-voltage parameters of full-square n-type Czochralski-grown silicon (Cz-Si) BC-BJ solar cells with an edge length of 156 mm and wire-based metallization concept (see Fig. 1b) a unit-cell simulation is carried out. The three-dimensional conductive boundary based simulation tool *Quokka* [8] is used. A schematic of the simulated unit cell is shown in Fig. 2. Note, that solely the contact finger metallization is interrupted. The doping pattern features continuous lines. The width of the contact finger interruption is varied from $d_{FI} = 0$ mm to $d_{FI} = 3$ mm. The width of the simulated unit cell d_{UC} depends on the number of wires $\#W$, which is varied from $\#W = 10$ to $\#W = 30$. It is defined as the coefficient of wafer edge length and number of wires $d_{UC} = l_{cell}/\#W$. All relevant input parameters of the simulation are listed in Table 1. The values for the dark saturation current densities j_0 of the doped areas are based on published values by Keding *et al.* for a co-diffused BC-BJ solar cell [9, 10]. The dark saturation current densities of the metallized areas j_{0met} are taken from publications with screen-printed n-type Cz-Si H-Pattern solar cells where the emitter contact is realized with a silver-aluminum paste and the BSF contact with a silver paste [11–13].

The series resistance contribution of the lateral current flow in the contact fingers of both polarities is calculated using the analytical expressions from [14, 15]:

$$r_f = \frac{2}{3} R_L \left(d_{UC} - \frac{d_{FI}}{2}\right) \cdot d_{UC} \frac{p}{2} . \qquad (1)$$

The series resistance contribution of the lateral current flow in the wires is calculated according to [16],

$$r_w = \frac{2}{3} \rho_{wire} \frac{l_{cell}{}^2}{\pi r_{wire}{}^2} d_{UC} . \qquad (2)$$

The calculated series resistances r_f and r_w are added and considered as a lumped series resistance $r_{s,lumped}$ for the *Quokka* simulation.

B. Adhesion Tests

Three groups of metallized BC-BJ solar cell dummies with different metallization layouts are fabricated according to Fig. 4. As base material, we use pseudo-square n-type Cz-Si wafers with an edge length of 156 mm, a diameter of 200 mm, and an initial thickness of 200 µm. Following alkaline saw-damage etching, an 80 nm-thick dielectric layer stack is deposited. On top, a commercial firing-trough silver paste is screen-printed applying 207 contact fingers with a pitch of 750 µm and a screen opening of 100 µm. In case of group 1 and group 2, continuous contact fingers are printed, whereas for group 3, an adopted layout with periodic contact finger interruptions is used. Subsequently, the samples are fired in an industrial fast firing furnace. Finally, a low-temperature insulation paste and a low-temperature copper-based busbar paste is screen-printed and thermally cured in case of the multi-layer metallization groups 1 and 2.

Group 1 features a layout with in total 8 continuous busbars (4 for each polarity) measuring 1.5 mm in width featuring round contact pads measuring 2 mm in diameter. In case of group 2, a 15 busbar layout consisting of rectangular contact pads each with an area of 2x11 mm² is applied. The wire-based metallization layout of group 3 has 30 contact pad rows. Every contact finger features a small solder pad. The width of the pad is $w_{\mathrm{pad,p}} = 400$ µm in case of the p-type pads, and $w_{\mathrm{pad,n}} = 200$ µm for the n-type pads. The pad length is varied along the wafer from $l_{\mathrm{pad}} = 0.5$ mm to $l_{\mathrm{pad}} = 1$ mm. The width of the contact finger interruption is $d_{\mathrm{FI}} = 1.5$ mm.

Three different types of solar cell interconnectors are soldered manually on the metallized dummies:

- 1 mm wide Sn62Pb36Ag2 alloyed copper ribbon (thickness 180 µm), solder coating about 18.3 µm
- 1.5 mm wide Sn62Pb36Ag2 alloyed copper ribbon (thickness 150 µm), solder coating about 19.0 µm
- Sn62Pb36Ag2 alloyed copper wire with a diameter of 270 µm, homogenous solder coating about 10 - 11 µm

Peel force measurements [17] are carried out using a Zwick tensile testing machine modified for 90°-peel testing.

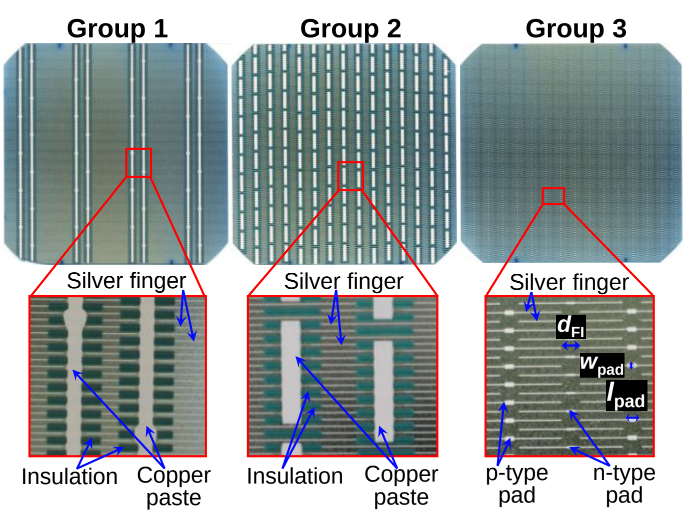

Fig. 4. Photographs of the rear side of the fabricated BC-BJ solar cell dummies with an edge length of 156 mm. Group 1 and 2 feature the multi-layer metallization concept shown in Fig. 1a, and group 3 the wire-based metallization concept shown in Fig. 1b.

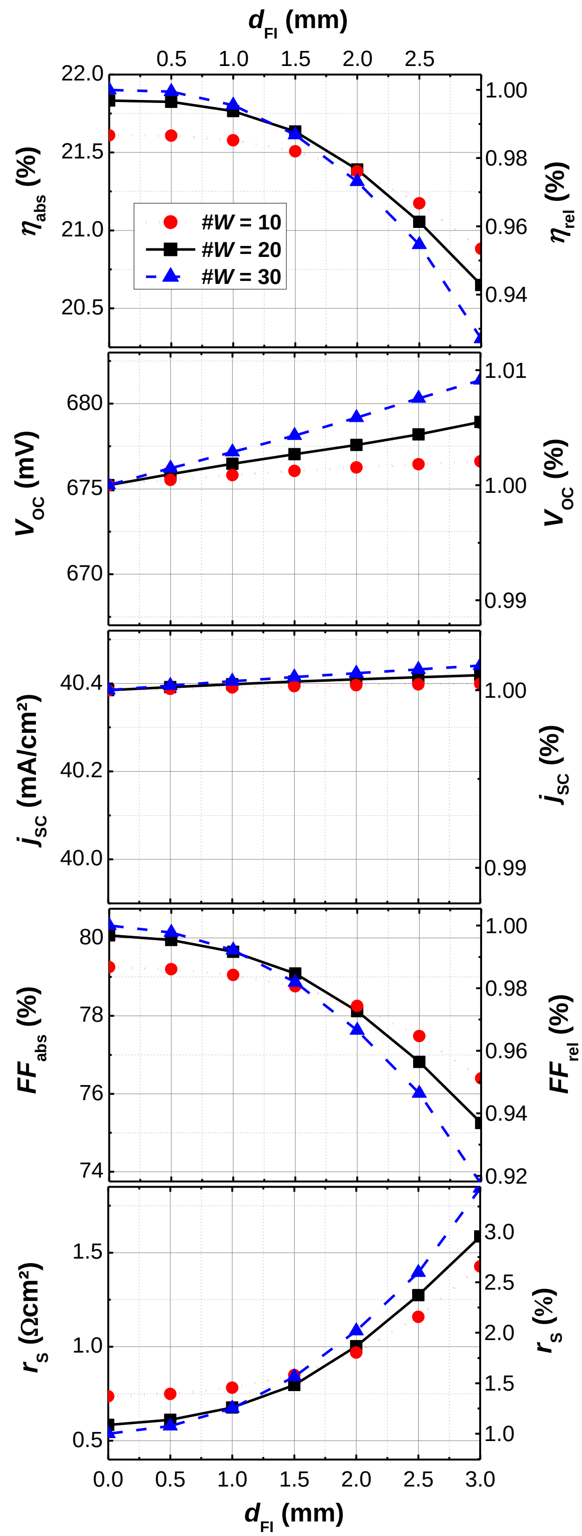

Fig. 3. Simulated solar cell parameters of n-type Cz-Si BC-BJ solar cells with an edge length of 156 mm and different wire-based metallization layouts. The right y-axis is standardized to a solar cell with $d_{\mathrm{FI}} = 0$ mm and $\#W = 30$. The corresponding *Quokka* unit cell is shown in Fig. 2.

III. Results and Discussion

A. Simulation of Wire-Based Cell Metallization Layouts

Fig. 3 shows the simulated solar cell parameters conversion efficiency η, open-circuit voltage V_{OC}, short-circuit current j_{SC}, fill factor FF, and series resistance r_S of n-type Cz-Si BC-BJ solar cells with an edge length of 156 mm with different number of wires $\#W$ and contact finger interruption width d_{FI}. The series resistance is calculated according to the double light method at the point of maximum power [18].

The efficiency loss with increased d_{FI} is mainly driven by the resistive losses, which results from increased lateral current path lengths in the non-metallized BSF and emitter regions. Due to a decrease of the metallized area fraction and thus reduced j_{0met} contributions, a slight V_{OC} gain is observed with increasing d_{FI}. Nevertheless, this gain is completely overcompensated by increased r_S losses. Metallization layouts with a higher number of wires $\#W$ show a sharper r_S raise with increasing d_{FI}, since in this case the total number of contact finger interruptions of the cell is larger.

The results show that the overall conversion efficiency drop of layouts with contact finger interruption with $d_{FI} \leq 1$ mm is below 0.1 % absolute when compared to $d_{FI} = 0$ mm for all investigated numbers of wires $\#W$. Calculating with a reasonable number of wires of $\#W = 30$ the efficiency drop amounts to $\Delta\eta = 0.096\ \%_{abs} = 0.450\ \%_{rel}$. Considering that the contact finger interruption allows for simplifying the BC-BJ solar cell back-end process sequence, the wire-based metallization concept appears as a very promising candidate for BC-BJ solar cells.

B. Adhesion Tests

Fig. 5 shows the results of the adhesive force measurements for all groups. In order to compare the different interconnector dimensions, the measured adhesive force F is normalized to the width of the solder joint specifying the normalized adhesive force F_N. In case of the ribbons, the width of the solder joint is equal to the ribbon width. For the wires, a solder joint width of 330 µm is assumed. The continuous line at $F_N = 1$ N/mm marks the standard threshold defined in the current industry norm [19]. For group 1 and 2, the average normalized force $ØF_N$ along the low-temperature busbar of three peel-force measurement strips is shown in the graph (see Fig. 5a and 5b). In case of group 3, the average normalized peak force $ØF_N^P$ between solder pad and wire is calculated from three strips averaging the peak forces of each measurement along the busbar according to reference [17] (see Fig. 5c).

In case of group 1, the highest average adhesive force of $ØF_N = 0.7$ N/mm is reached with 1 mm wide soldered ribbons. The analysis of the samples after peel testing reveal a homogenous cohesive fracture in the low-temperature copper-based busbar metallization. The adopted busbar shape of group 2 results in slightly higher average adhesive forces of

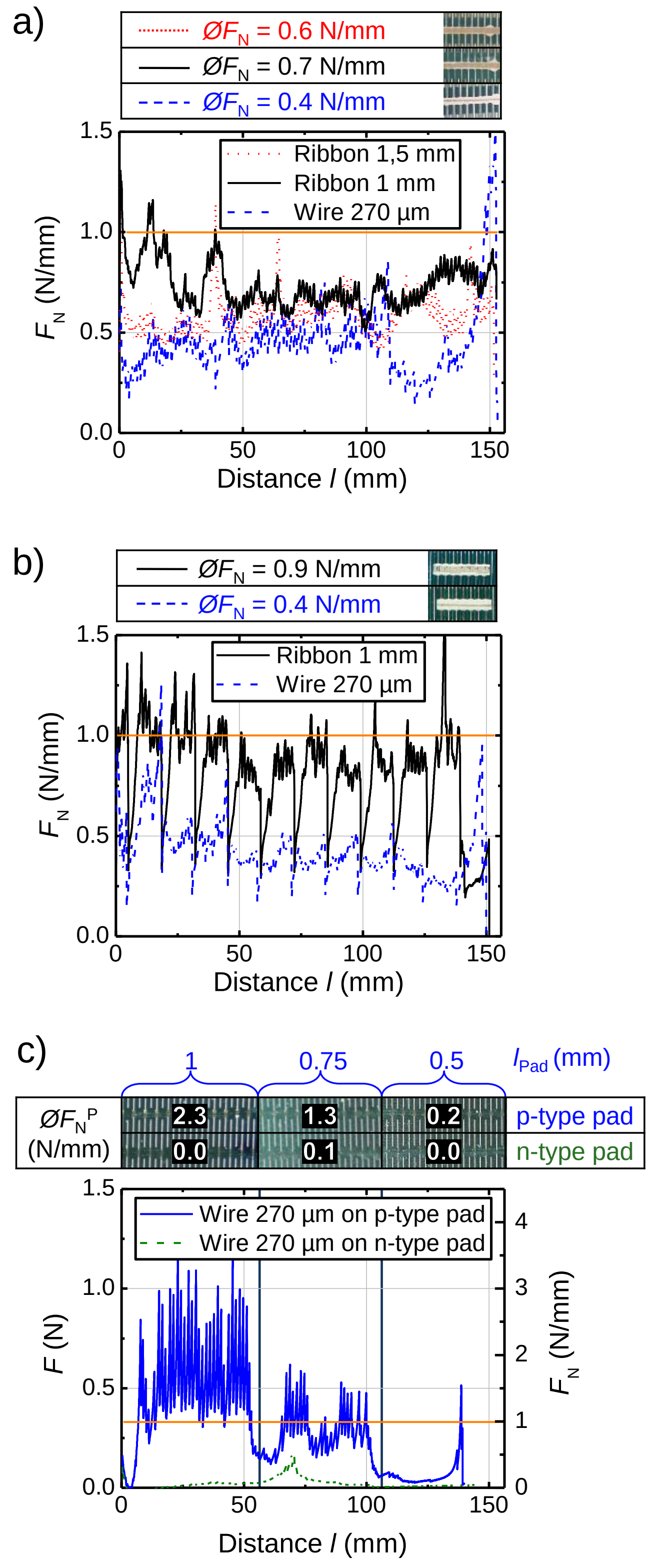

Fig. 5. Measured adhesive force F_N between soldered cell interconnector and solar cell metallization along one exemplary busbar for a) group 1, b) group 2, and c) group 3 according to Fig. 3 for different interconnector dimensions. The pictures show exemplary contact pads after the adhesion test. The average values $ØF_N$ and $ØF_N^P$ are calculated from three measurement strips per group.

$ØF_N = 0.9$ N/mm using a 1 mm wide ribbon. In addition to the cohesive fracture of the busbar paste, an adhesive fracture is visible at the interface between rear passivation layer and busbar paste.

However, for both groups the weakest link of the multi-layer stack is the low-temperature copper-based busbar paste. The measured average adhesive forces are rather low compared to an industrial three busbar H-Pattern solar cell with silver-based high-temperature paste and 1.5 mm wide ribbon, where we achieve $ØF_N = 2.7$ N/mm under identical soldering conditions.

The results of group 3 with wire-based metallization concept clearly show that the pad geometry of the firing-trough silver paste is a crucial parameter for the peel force of the wire-based metallization concept with soldered cell interconnectors. The width of the n-type pads $w_{pad,n} = 200$ µm is too small in order to achieve a sufficient adhesion, resulting in peel forces well below the required 1 N/mm. In case of the wider p-type pads with $w_{pad,p} = 400$ µm, adhesion forces of $ØF_N^P > 1$ N/mm are reached for $l_{pad} \geq 0.75$ mm. The highest average normalized peak force of $ØF_N^P = 2.3$ N/mm is achieved on solder pads with $l_{pad} = 1$ mm and $w_{pad,p} = 400$ µm. This value is close to the industrial benchmark (H-Pattern with 3 busbars) with $ØF_N = 2.7$ N/mm.

IV. Conclusion

In this study, we investigate two different metallization concepts for large-area screen-printed n-type Cz-Si BC-BJ solar cells: i) a multi-layer concept with screen-printed copper-based low-temperature busbars, and ii) a wire-based concept with interrupted silver contact finger metallization.

The effect of the contact finger interruption is simulated by means of three-dimensional numerical simulations. The results show that contact finger interruptions up to $d_{FI} = 1$ mm result in non-significant conversion efficiency drop of $\Delta\eta < 0.1$ % absolute for metallization layouts with 30 wires. This is a promising value, since we consider $d_{FI} = 1$ mm as the lower limit for a reliable wire-based module assembly process in industrial environment. From a cost-benefit perspective, the wire-based metallization concept is of high interest, since it allows for omitting two screen printing processes at the end of the solar cell manufacturing compared to the multi-layer concept.

For both investigated concepts, we found metallization layouts for 156 mm solar cells that reach sufficiently high peel forces $ØF_N$ applying conventional soldering technology. In case of the copper-based low-temperature busbars with printed insulation layer beneath, maximum average values of $ØF_N = 0.9$ N/mm are reached for the investigated 15 busbar multi-layer concept. By a further optimization of the busbar design or by changing the low-temperature busbar paste, we expect to achieve values exceeding the industrial norm of $ØF_N = 1$ N/mm. For the wire-based metallization approach with interrupted contact fingers, a minimum contact finger pad width $w_{pad} = 0.4$ mm and a length ≥ 0.75 mm are found in order to achieve sufficiently high peel forces of > 1 N/mm to soldered wires.

Acknowledgement

The authors thank all colleagues at the Fraunhofer ISE Photovoltaic Technology Evaluation Center (PV-TEC) for their support; especially E. Lohmüller, M. Retzlaff and V. Krumm as well as S. Hoffmann from Photovoltaic Module Technology Center. The work was supported by the European Union's Seventh Programme for research, technological development and demonstration under grant agreement No 608498 (project "Hercules") and by the German Federal Ministry for Economic Affairs and Energy under contract number 0325491 (project "Thesso").

References

[1] K. Masuko, M. Shigematsu, T. Hashiguchi, D. Fujishima, M. Kai, N. Yoshimura, T. Yamaguchi, Y. Ichihashi, T. Mishima, N. Matsubara, T. Yamanishi, T. Takahama, M. Taguchi, E. Maruyama, and S. Okamoto, "Achievement of More Than 25% Conversion Efficiency With Crystalline Silicon Heterojunction Solar Cell," *IEEE J. Photovoltaics*, vol. 4, no. 6, pp. 1433–1435, 2014.

[2] D. D. Smith, P. J. Cousins, A. Masad, S. Westerberg, M. Defensor, R. Ilaw, T. Dennis, R. Daquin, N. Bergstrom, A. Leygo, X. Zhu, B. Meyers, B. Bourne, M. Shields, and D. Rose, "SunPower's Maxeon Gen III solar cell: High efficiency and energy yield," in *2013 IEEE 39th Photovoltaic Specialists Conference (PVSC)*, pp. 0908–0913.

[3] G. Galbiati, V. D. Mihailetchi, R. Roescu, A. Halm, L. J. Koduvelikulathu, R. Kopecek, K. Peter, and J. Libal, "Large-Area Back-Contact Back-Junction Solar Cell With Efficiency Exceeding 21%," pp. 560–565.

[4] M. Hendrichs, R. Keding, T. Fellmeth, A. Spribille, and F. Clement, "Optimization of multi-layer metallization design for large-area back-contact back-junction solar cells," *Proc. 29th EU-PVSEC*, pp. 412–416, 2014.

[5] S. Braun, G. Micard, and G. Hahn, "Solar Cell Improvement by using a Multi Busbar Design as Front Electrode," *Energy Procedia*, vol. 27, pp. 227–233, 2012.

[6] A. Schneider, L. Rubin, and G. Rubin, "Solar Cell Efficiency Improvement by New Metallization Techniques - the Day4 Electrode Concept," in *2006 IEEE 4th World Conference on Photovoltaic Energy Conference*, pp. 1095–1098.

[7] G. Hahn, B. Raabe, and F. Book, "Busbarless Rear-Contact Solar Cell, Method of Manufacture therefore and Solar Module Having such Solar Cells", WO 2014/124675 A1.

[8] A. Fell, K. Fong, and K. McIntosh, "3-D Simulation of Interdigitated-Back-Contact Silicon Solar Cells With Quokka

Including Perimeter Losses," *IEEE J. Photovoltaics*, vol. 4, no. 4, pp. 1040–1045, 2014.

[9] R. Keding, M. Hendrichs, D. Stüwe, M. Jahn, C. Reichel, D. Borchert, A. Wolf, H. Reinecke, and D. Biro, "POCL3-Based Co-Diffused Process for n-type Back-Contact Back-Junction Solar Cells," *Proc. 29th EU-PVSEC*, pp. 677–680, 2014.

[10] R. Keding, D. Stüwe, M. Kamp, C. Reichel, A. Wolf, R. Woehl, D. Borchert, H. Reinecke, and D. Biro, "Co-Diffused back-Contact Back-Junction Silicon Solar Cells," *Proc. 28th EU-PVSEC*, pp. 961–966, 2013.

[11] T. Fellmeth, A. Born, A. Kimmerle, F. Clement, D. Biro, and R. Preu, "Recombination at Metal-Emitter Interfaces of Front Contact Technologies for Highly Efficient Silicon Solar Cells," *Energy Procedia*, vol. 8, pp. 115–121, 2011.

[12] A. Edler, V. D. Mihailetchi, L. J. Koduvelikulathu, C. Comparotto, R. Kopecek, and R. Harney, "Metallization-induced recombination losses of bifacial silicon solar cells," *Prog. Photovolt: Res. Appl,* vol. 23, no. 5, pp. 620–627, 2015.

[13] E. Lohmüller, S. Werner, B. Thaidigsmann, N. Wöhrle, S. Mack, F. Clement, and D. Biro, "The HIP-MWT+ Solar Cell Concept on n-type Silicon and Metallization-Induced Voltage Losses," *Proc. 29th EU-PVSEC*, pp. 635–641, 2014.

[14] T. Fellmeth, F. Clement, and D. Biro, "Analytical Modeling of Industrial-Related Silicon Solar Cells," *IEEE J. Photovoltaics*, vol. 4, no. 1, pp. 504–513, 2014.

[15] A. Goetzberger, B. Voß, and J. Knobloch, Eds, *Sonnenenergie: Photovoltaik - Physik und Technologie der Solarzelle,* 2nd ed, 1997.

[16] S. Braun, "Simulation, Analyse und Herstellung von kristallinen Si-Solarzellen mit Multi-Busbar-Verschaltung," Dissertation, Universität Konstanz, Konstanz, 2014.

[17] J. Walter, M. Tranitz, M. Volk, C. Ebert, and U. Eitner, "Multi-wire Interconnection of Busbar-free Solar Cells," *Energy Procedia*, vol. 55, pp. 380–388, 2014.

[18] P. P. Altermatt, G. Heiser, A. G. Aberle, A. Wang, J. Zhao, S. J. Robinson, S. Bowden, and M. A. Green, "Spatially resolved analysis and minimization of resistive losses in high-efficiency Si solar cells," *Prog. Photovolt: Res. Appl,* vol. 4, no. 6, pp. 399–414, 1996.

[19] *DIN EN 50461*, Solar cells - Datasheet information and product data for crystalline silicon solar cells, German version EN 50461, 2006.